Published in IET Generation, Transmission & Distribution
Received on 7th February 2013
Revised on 5th September 2013
Accepted on 12th September 2013
doi: 10.1049/iet-gtd.2013.0099

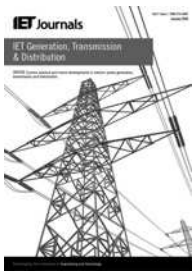

ISSN 1751-8687

Design and experimental evaluation tests of a Takagi–Sugeno power system stabiliser

Fabrício G. Nogueira[1], Walter Barra Jr.[2], Carlos T. da Costa Jr.[2], Anderson R. B. de Moraes[2], Marcus C. M. Gomes[2], Janio J. de Lana[3]

[1]*School of Electrical Engineering, Universidade Federal do Ceará (UFC), CT, Fortaleza, CE 60020-181, Brazil*
[2]*School of Electrical Engineering, Universidade Federal do Pará (UFPA), ITEC, Belém, PA 66075-110, Brazil*
[3]*Centrais Elétricas do Norte do Brasil (Eletronorte), Tucuruí Hydroelectric Power Plant, Tucuruí, PA 66033640, Brazil*
E-mail: walbarra@ufpa.br

Abstract: In this study, the design, implementation and experimental evaluation tests of a Takagi–Sugeno power system stabiliser (TSPSS) controller is presented. The controller was designed in order to provide a good damping for dominant electromechanical oscillations in power systems for the set of allowed operating conditions. In the proposed TSPSS controller, such requirement was accomplished by implementing a supervision scheme which performs the adaptation of the TSPSS parameters at each sample time, according to the current detected plant operating condition. The TSPSS controller has been implemented as a microcontroller-based embedded system and its performance was assessed by performing experimental tests in a laboratory scale (10 kVA) power system as well as in field tests performed in a large (350 MVA) generating unit, at Tucuruí Hydroelectric Power Plant. The experimental results also show the good performance of the TSPSS to cope with varying plant operation condition.

1 Introduction

Electromechanical oscillations are natural phenomena which occur in electrical power systems having interconnected generators. Poorly damped electromechanical oscillation modes are extremely undesirable for the operation of power systems, because they can considerably limit the power transfer between interconnected generating areas. Furthermore, poorly damped electromechanical oscillations can also decrease the lifetime expectancy of the power system machines. Among electromechanical oscillation modes in power systems, the intra-plant oscillation mode is the one which arises from interactions between unit generators in a given power plant [1]. Therefore, in order to obtain safe plant operation, preserving machine life expectancy, a satisfactory damping of dominant intra-plant oscillation modes must be assured for all sets of allowed operating conditions.

In [1], the author presents a study of intra-plant modes as affected by power system stabiliser (PSS) tuning. The study was performed by computer simulation and modal analysis. It was concluded that a destabilising effect can be observed in plants having generators with similar parameters and control systems. Other early references have also already studied intra-plant modes for a two-generator power plant, including field tests [2]. In [3], a case study is shown where there is a considerable overlap between the range of frequencies of the local and intra-plant modes. Therefore a modal analysis study is necessary in order to classify an oscillation mode as local or intra-plant.

In [4], the performance of a digital controller, designed to damp the intra-plant oscillation modes observed between generating units at a thermal power plant, was assessed by field tests. It was shown that the digital controller was able to provide sufficient damping for the dominant intra-plant oscillation mode, for all allowed plant operating conditions. In [5], a software simulation tool was designed with the purpose of reproducing observed intra-plant oscillations at a large Brazilian hydroelectric power plant. To that end, quite detailed modelling for each individual generating unit was carried out.

Therefore, in order to improve system reliability and assure safe operation, the dominant electromechanical oscillation modes should be satisfactorily damped by using adequate automatic control techniques. Usually, PPS controllers are used in order to increase the damping of observed dominant electromechanical oscillation modes. A PSS controller acts as a secondary controller, modulating the reference of the automatic voltage regulator (AVR) of the generating unit in order to increase the damping of the target electromechanical oscillation mode [1]. Nowadays, the research in new improved strategies for damping controller design and implementation is still in progress and new topologies, such as the two-band (PSS2B) and the multiband PSS (named PSS4B), which has been proposed and evaluated in [6].

The tuning of PSS controllers is still based on the use of classical linear control techniques leading to a fixed-gain linear PSS controller structure. However, because of the non-linear and time-variable behaviour of electrical power

systems, fixed-gain linear PSS controllers may lose their performance, dangerously reducing the power system stability margins.

To cope with the time-variable nature of the power system operation, a considerable research effort has been carried out over the past three decades on the investigation of adaptive PSS control strategies. These adaptive strategies aim to cope with controller detuning because of time-variable operating conditions in power systems. The adaptive methodologies investigated include: self-tuning control [7], robust-optimal control [8–10], fuzzy [11] and fuzzy-neural techniques [12], among others. In [11], a fuzzy logic PSS (FLPSS) was designed and its performance was assessed, by simulation studies, in a four-machine test system. The authors show that the performance obtained by using the FLPSS was comparable with the obtained when applying PSS2B or PSS4B controllers. However, no experimental tests were performed in a real power system. A natural approach to dealing with changes in the plant operating point is the gain scheduled methodology [13]. In this kind of adaptive strategy, the PSS controller gain adjustment is performed by a supervisory scheme, according to the detected changes in the current plant operating conditions.

The design, development and field tests of a Takagi–Sugeno PSS (TSPSS) are presented and discussed hereby. The control strategy is based on a fuzzy supervisory scheme which performs a weighted average among the output response of pre-designed local PSS controllers, according to the current plant operating conditions. The fuzzy supervision scheme aims to keep the damping controller well-tuned in spite of variations in the plant operating conditions.

The evaluation of the proposed TSPSS damping controller was performed in laboratory as well as in field tests at a large Brazilian hydroelectric power plant (Tucuruí Power Plant). The field test objective was to damp a dominant intra-plant oscillation mode observed between the 350 MVA generating units of that power plant. It is worth emphasising that, currently, there are just a few papers presenting practical results in large power plants. Therefore, the authors believe that the main contribution from this paper is to show a systematic design methodology for an adaptive fuzzy controller, along with its field tests in a large generating unit. The steps and challenges involved in the implementation of the TSPSS controller, as well as in executing field evaluation tests in a large power plant, are also discussed.

This paper is organised as follows: in Section 2, the proposed adaptive fuzzy PSS methodology is presented. Section 3 presents the development of the controller hardware. The laboratory tests results are presented and discussed in Section 4. The results of the field tests for the TSPSS controller are presented and discussed in Section 5. The conclusions of this study are provided in Section 6.

2 TSPSS design and implementation methodology

2.1 Introduction

In this section, the adaptive methodology used in the design and implementation of the TSPSS is described. The Takagi–Sugeno (TS) modelling approach can be very useful in industry and electrical power system applications because it allows for modelling the dynamic behaviour of the plant system operating around a set of allowed operating

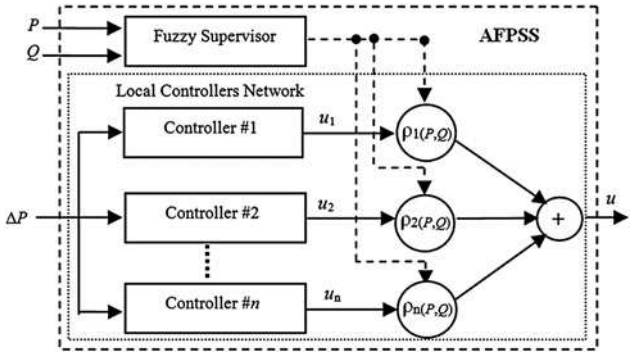

Fig. 1 *Representative block diagram of the TSPSS*

conditions by using local linear models, which are merged by using weighting membership functions usually obtained from qualitative plant knowledge. The modelling of the important system non-linearities is by performed using membership function of selected scheduling variables, which define the plant operating conditions. Therefore the whole TS model embedded both linear and non-linear available plant information.

As illustrated in Fig. 1, the controller is comprised of a set of linear local controllers, the individual outputs of which are interpolated by using a fuzzy supervision scheme.

The values of the active (P) and reactive powers (Q), measured at the machine terminal, are used as the scheduling variables for the fuzzy supervision scheme. Therefore those local controllers whose design operating points are 'closer' to the actual plant operating point (in a fuzzy sense) will have a dominant contribution to the composition of the response of the TSPSS controller. As can be seen in Fig. 1, the contribution of each local controller to the TSPSS global response is weighted by a set of operating point-dependent weight factors, assuming values in the real interval [0, 1].

2.2 Designing the local controllers using the pole shifting technique

For each operating point selected for designing the local controllers, the parameters of a linear autoregressive with exogenous input (ARX) model

$$\frac{B(q^{-1})}{A(q^{-1})} = \frac{b_1 q^{-1} + b_2 q^{-2} + \cdots + b_{nB} q^{-nB}}{1 + a_1 q^{-1} + a_2 q^{-2} + \cdots + a_{nA} q^{-nA}} \quad (1)$$

are estimated by using traditional identification techniques [14], where nB and nA are, respectively, the orders of the polynomials of the numerator and denominator of the model. Subsequently, by using pole-placement techniques [15], the parameters of a corresponding minimum order local controller having the standard form

$$\frac{R(q^{-1})}{S(q^{-1})} = \frac{r_0 + r_1 q^{-1} + r_2 q^{-2} + \cdots + n_{nR} q^{-nR}}{1 + s_1 q^{-1} + s_2 q^{-2} + \cdots + s_{nS} q^{-nS}} \quad (2)$$

are calculated by solving the following linear system of

doi: 10.1049/iet-gtd.2013.0099

equations

$$\begin{bmatrix} 1 & 0 & . & 0 & b_1 & 0 & . & 0 \\ a_1 & 1 & . & 0 & b_2 & b_1 & . & 0 \\ . & a_1 & . & . & . & b_2 & . & . \\ a_{n_A} & . & . & 1 & b_{n_B} & . & . & b_1 \\ 0 & a_{n_A} & . & a_1 & 0 & b_{n_B} & . & b_2 \\ . & 0 & . & 0 & . & 0 & . & . \\ . & . & . & . & . & . & . & . \\ 0 & 0 & . & a_{n_A} & 0 & 0 & . & b_{n_B} \end{bmatrix} \begin{bmatrix} s_1 \\ . \\ . \\ s_{n_S} \\ r_0 \\ . \\ . \\ r_{n_R} \end{bmatrix} = \begin{bmatrix} (\alpha - 1)a_1 \\ (\alpha^2 - 1)a_2 \\ . \\ . \\ (\alpha^{n_A} - 1)a_{n_A} \\ 0 \\ . \\ 0 \end{bmatrix} \quad (3)$$

where α, the radial contraction factor, is calculated by using

$$\alpha = \mathrm{e}^{-(\zeta_\mathrm{d} - \zeta)\omega_n T_\mathrm{s}} \quad (4)$$

In (7), ζ and ω_n are, respectively, the relative damping and the natural angular frequency of the target oscillation mode, T_s is the control interval and ζ_d is the desired value for the damping of the oscillation mode, which must be specified by the designer.

The pole-shifting method was used to tune all the linear controllers to be scheduled by the fuzzy supervision scheme (see Fig. 1). Therefore, in the next two sections, the theoretical and practical aspects of the fuzzy supervisor will be discussed.

2.3 Fuzzy supervisory scheme

A TS fuzzy supervisor performs the average between the output responses of the local controllers, according to the continuous variation of the operational conditions of the system. The characterisation of the plant operating point is defined by the values of active power, $P(t)$, and reactive power, $Q(t)$, measured at the generating unit terminals. Based on the practical knowledge of the power plant operation, the $P \times Q$ operating plane was partitioned into nine operating regions (Fig. 2*a*) and, for each region, a corresponding local controller was designed, by using the methodology of the Section 2.2. It is worth remarking that the closed-loop performance can be improved by selecting an increased number of local controllers. However, this has the drawback of leading to an increased execution time for the control law calculation, as well as demanding the execution of identification tests in a larger set of operating conditions.

To qualitatively characterise the operation variables P and Q, triangular membership functions were used, as can be seen in Figs. 2*b* and *c*. Therefore, by combining the chosen fuzzy sets for both schedule variables, P and Q, a rule base having nine rules can be obtained. By using the inference product for the membership functions of the fuzzy sets of $P(t)$ and $Q(t)$, the corresponding weight for each rule is obtained, as shown in the equation system (5).

$$\begin{cases} \rho^{(1)} = \mu_{\text{negative}}(P).\mu_{\text{low}}(Q) \\ \rho^{(2)} = \mu_{\text{negative}}(P).\mu_{\text{medium}}(Q) \\ \rho^{(3)} = \mu_{\text{negative}}(P).\mu_{\text{high}}(Q) \\ \rho^{(4)} = \mu_{\text{zero}}(P).\mu_{\text{low}}(Q) \\ \rho^{(5)} = \mu_{\text{zero}}(P).\mu_{\text{medium}}(Q) \end{cases} \text{and} \quad \begin{cases} \rho^{(6)} = \mu_{\text{zero}}(P).\mu_{\text{high}}(Q) \\ \rho^{(7)} = \mu_{\text{positive}}(P).\mu_{\text{low}}(Q) \\ \rho^{(8)} = \mu_{\text{positive}}(P).\mu_{\text{medium}}(Q) \\ \rho^{(9)} = \mu_{\text{positive}}(P).\mu_{\text{high}}(Q) \end{cases} \quad (5)$$

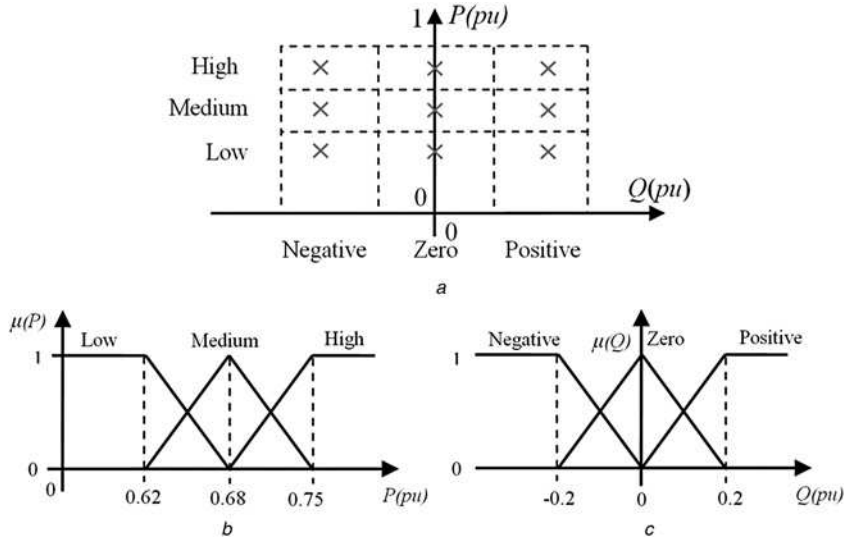

Fig. 2 *Fuzzy supervisory scheme*

a Partition of the $P \times Q$ plane
b Pertinence functions of active and
c Reactive power

where the membership functions are $\mu_{negative}(.)$, $\mu_{zero}(.)$, $\mu_{positive}(.)$, for both $P(t)$ and $Q(t)$. Therefore, at a given instant, the resulting values of $\rho^{(l)}$ determine the contribution of each local controller ($R^{(l)}$ and $S^{(l)}$) for the composition of the values of the global fuzzy controller parameters (R' and S'), determining the value of fuzzy PSS controller output, (u). In this way, the parameters of the fuzzy PSS controller are calculated by using (6) and (7).

$$r'_n = \rho^{(1)} r_n^{(1)} + \rho^{(2)} r_n^{(2)} + \cdots + \rho^{(l)} r_n^{(l)}, \quad n = 0, 1, \ldots, n_r \tag{6}$$

$$s'_n = \rho^{(1)} s_n^{(1)} + \rho^{(2)} s_n^{(2)} + \cdots + \rho^{(l)} s_n^{(l)}, \quad n = 1, \ldots, n_s \tag{7}$$

As can be seen, the coefficients of the TSPSS controller depend on both the coefficients of the local controllers and the values of the inferences of the membership functions assumed in a certain operating point of the system. At each sample time, the coefficients of the TSPSS controller are updated by calculating a weighted sum of the coefficients of the local controllers, by using (6) and (7). The values of parameters of the local controllers are previously stored in the microcontroller data memory. The weight values, $\rho^{(l)}$, in (6) and (7), are variables which depends on the current operating condition (the values of P and Q) and are updated at each sample time, by using (5).

3 Hardware development

The digital PSS was implemented in an embedded system based on a digital signal controller, DSPIC30f5011, which has many integrated peripherals, digital signal processing capacity and can be coded in C language.

The signals that represent the nominal values of the machine variables were measured using an instrument called a PQVI transducer, which provides analogue signals proportional to the active power, reactive power and root-mean-square value of terminal voltage of the synchronous machine. These signals are previously processed by conditioning electronic circuits in order to perform the filtering of noise and transform the voltage levels according to the input limits of the A/D converter (ADS8345) used.

The numerical value of the output control signal, generated by the control law embedded in the DSPIC, is converted to an analogue signal conditioned to a ±1 VDC range, before applying it into an analogue input of the AVR. To perform system parameterisation and operation monitoring, a human–machine interface is available which allows for the storage and real-time visualisation of the plant's input and output data collected.

4 Experimental evaluation of the TSPSS controller in a reduced-scale power system

In this section, the results of the experimental performance evaluation of the developed TSPSS controller are presented. The tests were carried out in a reduced-scale power system, located at Federal University of Pará (UFPA), Brazil. By safety reasons, it is advisable to perform controller tests in a reduced-scale power system before performing field tests on large electrical generator systems. Furthermore, by using a laboratory-type power system it becomes easier to change the operating conditions in a controlled way. This feature allows for repeating the tests many times, and under different operating conditions, which is normally necessary for research purposes.

4.1 Description of the 10 kVA study power system

The laboratory power system is comprised of a synchronous generating unit (10 kVA, 220 V_{rms}, 60 Hz), a transmission line model, transformers, as well as measurement and control subsystems (Fig. 3*a*). The system has a typical machine-infinite bus bar power system configuration (Fig. 3*b*). The synchronous generator was built in order that its physical parameter values are similar, in per unit values, to that of large synchronous generators. An inductive represents a typical short transmission line. The values for the synchronous generator parameters are provided in Table 1. The values for resistances of the transmission line model and transformers are, respectively, $R_e = 0.049$ pu, $X_e = 0.197$ pu, $X_t = 0.040$ pu. The system's base values, for both generator and network, are $S_{base} =$ 10 kVA, $V_{base} = 220$ V rms and $f_{base} = 60$ Hz. The synchronous generator unit is equipped with a fast-actuating field excitation system based on a DC–DC buck converter (Fig. 4). The AVR is of proportional type, having a high-gain value.

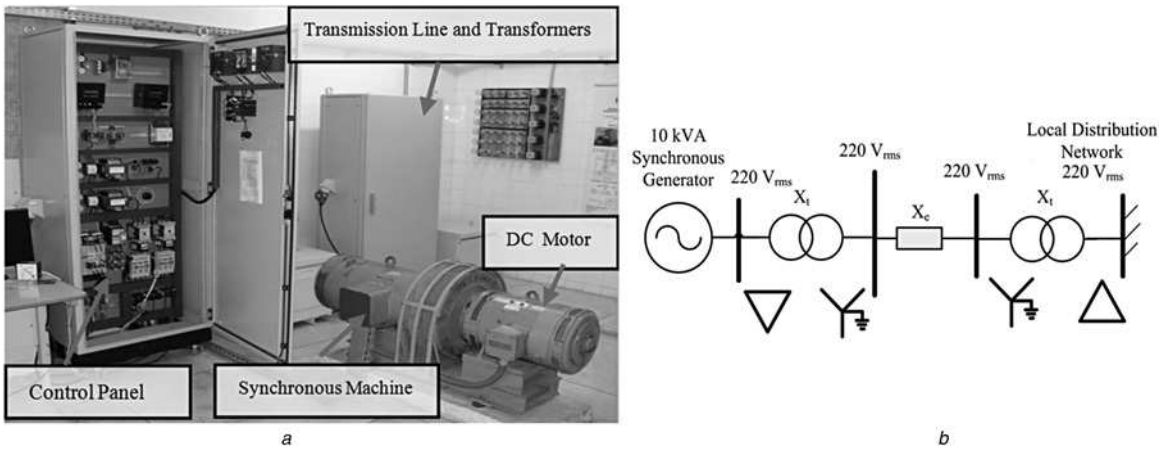

Fig. 3 *Reduced scale 10 kVA power system at UFPA*

doi: 10.1049/iet-gtd.2013.0099

Table 1 Parameter values for the synchronous generator

R_a,pu	X_d, pu	X_q, pu	X'_d, pu	X''_d, pu	X''_q, pu	T'_{d0}, s	T''_{d0}, s	T''_{q0}, s	H, s
0.048	1.058	0.693	0.169	0.0736	0.0736	0.490	0.019	0.019	3.861

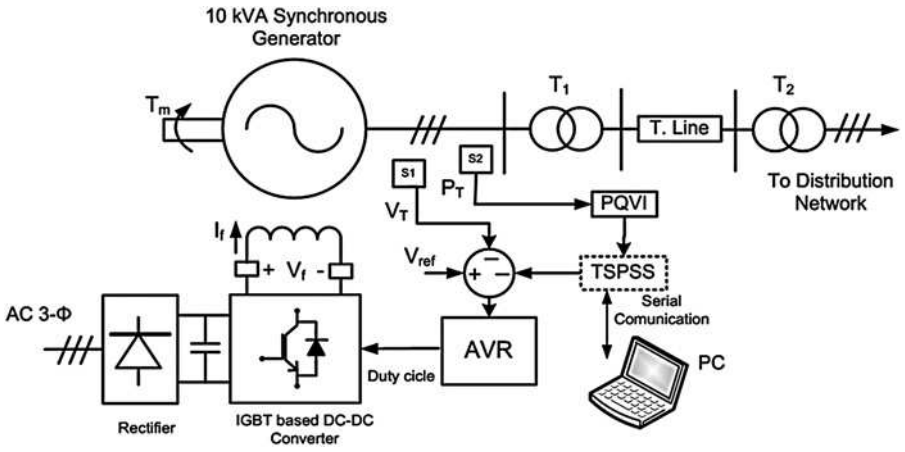

Fig. 4 *Scheme of connection for the TSPSS*

4.2 Evaluating the damping of the dominant electromechanical mode, without using a damping controller

For the system at the operating point $P_{TO} = 0.50$ pu, $V_{TO} = 1.000$ pu, $Q_{TO} \cong 0.00$ pu, and without using any damping controller, a 4% positive step variation was applied to the AVR set point, and the corresponding active power deviation response signal, ΔP_T, was acquired (Fig. 5*a*). It can be seen, from Fig. 5*a*, that, without using a PSS damping controller, the dominant electromechanical oscillation mode is poorly damped at the current operating condition. The period of the dominant oscillation can be estimated, from Fig. 5*a*, to be around $T_{osc} \simeq 0.80$ s. Therefore a sampling interval of $T_S = 0.060$ s (satisfying $T_S = T_{osc}$) was selected for acquisition and control purposes.

A pseudo-random binary sequence (PRBS) test signal, designed in order to excite uniformly the range of frequencies from 0.02 to 3.0 Hz, was applied into the summing point of AVR reference (see Fig. 4). The amplitude of the PRBS signal was selected small (0.01 pu) in order not to disturb the voltage control operation. The spectra estimated from the collected data are shown in Fig. 5*b*. It can be observed that the spectrum of the power deviation signal exhibits a dominant oscillating mode around 1.2 Hz, which corresponds to the poorly damped electromechanical local mode of the synchronous 10 kVA generator against the large power system.

By using the collected input–output data, a fourth order ARX model, having the structure presented in (11), was estimated. The values for the estimated parameters are provided in Table 2. Fig. 6 shows the comparison between the measured plant output signal and the output estimated by the identified ARX model. The good fit obtained by the estimated ARX model can be seen. Additional validation tests, based on the correlation of the residual, were also performed and confirmed the good performance of the identified model.

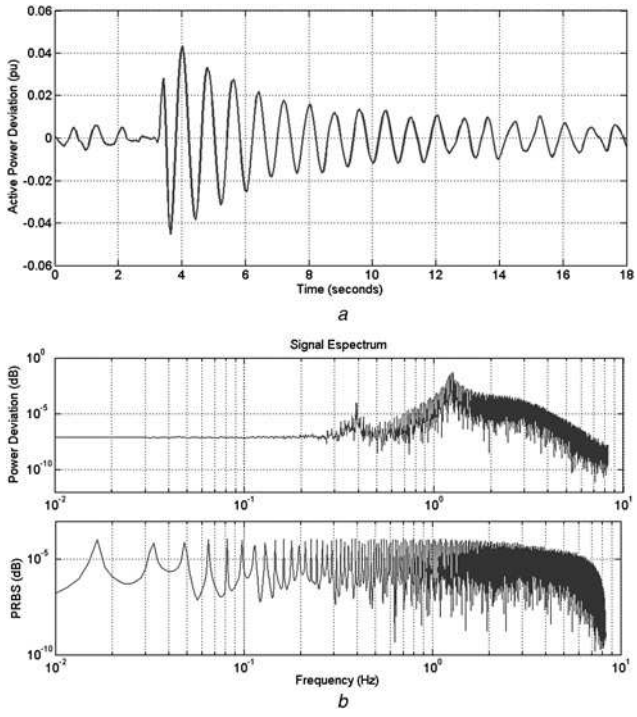

Fig. 5 *Evaluating the damping of the dominant electromechanical mode without using a damping controller*

a Step response for the power system operating without using PSS controller
b Estimate of the plant output spectrum, ΔP_T, and the PRBS test signals

$$\frac{B(q^{-1})}{A(q^{-1})} = \frac{q^{-2}\left(b_1 + b_2 q^{-1} + b_3 q^{-2} + b_4 q^{-2}\right)}{1 + a_1 q^{-1} + a_2 q^{-2} + a_3 q^{-3} + a_4 q^{-4}} \quad (8)$$

Table 2 Values of the parameters for the identified AXR model ($T_s = 60$ ms)

b_1	b_2	b_3	B_4	a_1	a_2	a_3	a_4
0.241621	−0.637356	0.129906	0.213117	−2.486382	2.796119	−1.662820	0.528979

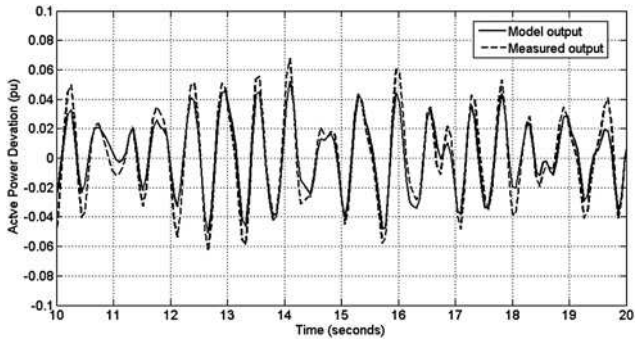

Fig. 6 *Comparison between the output of the identified ARX (solid line) and measured plant output (dashed line)*

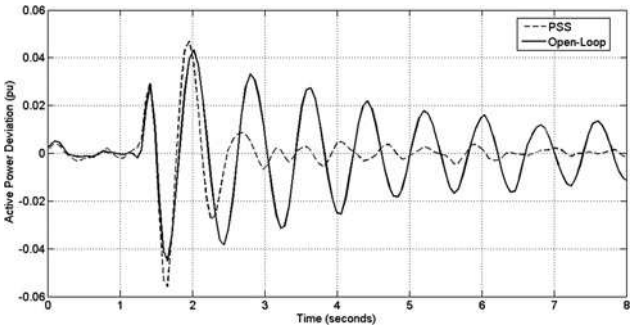

Fig. 7 *Step response test for the power system using the designed fixed-parameter PSS*

4.3 Designing a fixed-parameter PSS

The pole-shifting design technique, described in Section 2.3, was used for designing a fixed-parameter PSS in order to improve the damping of the electromechanical oscillation mode. By using the coefficients of the identified ARX model (Table 3), the following values for the relative damping and for the natural angular frequency were estimated for the system operating without PSS: $\zeta = 0.026$, $\omega_n = 7.86$ rad/s. Therefore, in order to improve the damping of the oscillating mode, a desired relative damping value of $\zeta_d = 0.30$ was specified for PSS design. By applying the (4), with a sample interval of $T_s = 0.060$ s, the corresponding value for the radial contraction factor was calculated as $\alpha = 0.8788$. The PSS controller structure is in the form of (13). The resulting values for the PSS parameters are provided in Table 3.

$$\frac{R(q^{-1})}{S(q^{-1})} = \frac{r_0 + r_1 q^{-1} + r_2 q^{-2} + r_3 q^{-2}}{1 + s_1 q^{-1} + s_2 q^{-2} + s_3 q^{-3} + s_4 q^{-4}} \qquad (9)$$

To evaluate the performance of the designed fixed-parameter PSS, a step response test was performed at the same operating condition ($P_{TO} = 0.50$ pu, $V_{TO} = 1.000$ pu, $Q_{TO} \cong 0.00$ pu). Fig. 7 shows the step response of the system for the system without PSS (solid line) and for the system using the designed fixed-parameter PSS (dashed line). The good performance of the designed fixed-parameter PSS can be observed, which was able to effectively damp the electromechanical oscillations, as required.

4.4 Designing and testing a TSPSS controller in order to cope with varying operating conditions

It is known that power system dynamics can change considerably with varying operating conditions. This may cause performance degradation in fixed-parameter PSS damping controllers. Therefore, in order to cope with varying operating conditions, a TSPSS controller was designed and its performance was compared with the one obtained by using the fixed-parameter PSS. Only to make the presentation of the main results easier, in all tests the selected scheduling variable was the generated active power, P_{T0}, whereas the terminal voltage was kept at its nominal value, $V_{T0} = 1.000$ pu, and the reactive power was kept close to zero ($Q_{T0} \simeq 0.00$ pu).

A set of three fuzzy rules, corresponding to the active power generation levels $P^{(1)} = \text{low}$, $P^{(2)} = \text{medium}$ and $P^{(3)} = \text{high}$, was defined according to (10). The membership

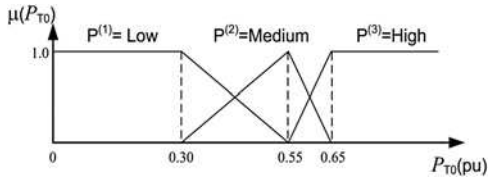

Fig. 8 *Membership functions for active power generation levels*

Table 3 Values of the parameters for the fixed PSS ($T_s = 60$ ms)

r_0	r_1	r_2	r_3	s_1	s_2	s_3	s_4
−0.653045	1.362027	−1.037801	0.528796	0.301333	0.270346	−0.381439	−0.213043

doi: 10.1049/iet-gtd.2013.0099

Table 4 Values of the parameters for the identified local AXR models ($T_s = 60$ ms)

P_{T0}, pu	b_1	b_2	b_3	b_4	a_1	a_2	a_3	a_4
0.30	0.219771	−0.552540	0.139379	0.157401	−2.500824	2.828090	−1.703784	0.546830
0.55	0.255502	−0.669889	0.141017	0.213774	−2.531436	2.886233	−1.734788	0.544769
0.65	0.286379	−0.705057	0.117853	0.218290	−2.468547	2.759580	−1.645278	0.526940

Table 5 Values of the parameters calculated for the TSPSS local controllers ($T_s = 60$ ms)

P_{T0}, pu	r_0	r_1	r_2	r_3	s_1	s_2	s_3	s_4
0.30	−0.882257	1.808377	−1.395093	0.717534	0.296546	0.304564	−0.424838	−0.206537
0.55	−0.619209	1.318267	−1.039116	0.520377	0.296459	0.272241	−0.377213	−0.204202
0.65	−0.477447	1.039607	−0.787144	0.427318	0.281557	0.238165	−0.322207	−0.177021

for the fuzzy sets $P^{(1)}$, $P^{(2)}$ and $P^{(3)}$, are provided in Fig. 8.

$$
\begin{aligned}
&R_1\text{:IF } P_{T0} \text{ IS } P^{(1)} \text{ THEN } \frac{R^{(1)}(q^{-1})}{S^{(1)}(q^{-1})} \\
&= \frac{r_0^{(1)} + r_1^{(1)}q^{-1} + r_2^{(1)}q^{-2} + r_3^{(1)}q^{-2}}{1 + s_1^{(1)}q^{-1} + s_2^{(2)}q^{-2} + s_3^{(3)}q^{-3} + s_4^{(4)}q^{-4}} \\
&R_2\text{:IF } P_{T0} \text{ IS} P^{(2)} \text{ THEN } \frac{R^{(2)}(q^{-1})}{S^{(2)}(q^{-1})} \\
&= \frac{r_0^{(2)} + r_1^{(2)}q^{-1} + r_2^{(2)}q^{-2} + r_3^{(2)}q^{-2}}{1 + s_1^{(2)}q^{-1} + s_2^{(2)}q^{-2} + s_3^{(2)}q^{-3} + s_4^{(2)}q^{-4}} \\
&R_3\text{:IF } P_{T0} \text{ IS } P^{(3)} \text{ THEN } \frac{R^{(3)}(q^{-1})}{S^{(3)}(q^{-1})} \\
&= \frac{r_0^{(3)} + r_1^{(3)}q^{-1} + r_2^{(3)}q^{-2} + r_3^{(3)}q^{-2}}{1 + s_1^{(3)}q^{-1} + s_2^{(3)}q^{-2} + s_3^{(3)}q^{-3} + s_4^{(3)}q^{-4}}
\end{aligned}
\tag{10}
$$

By using the same procedure as described in Section 4.2, three local ARX models were identified, corresponding to the selected operating points $P_{T0} = \{0.30, 0.55, 0.65\}$ pu. These operating points were chosen to be the respective centres of the selected fuzzy sets $P^{(1)} =$ low, $P^{(2)} =$ medium and $P^{(3)} =$ high, as illustrated in Fig. 8. The identified local models have the structure of (13) and were validated by using residual correlation tests. The estimated values for the parameters of local ARX models are provided in Table 4.

By using the estimated model parameter values, along with the specification of $\zeta_d = 0.30$, for the desired relative damping, the parameters of the TSPSS's local controllers were then calculated by using the pole-shifting technique. The resulting values for the parameters of the TSPSS's local controllers are provided in Table 5.

The performance of the designed TSPSS damping controller was evaluated to the performance obtained when using a fixed-parameter PSS. For the tests, the fixed-parameter PSS was the same controller designed in Section 4.3. Fig. 9 shows the results of the step response tests carried out for two different levels of active power generation: $P_{T0} = 0.60$ pu (Fig. 9*a*) and $P_{T0} = 0.70$ pu (Fig. 9*b*). The solid line is the step response for the plant under control of the designed TSPSS controller, whereas the dashed-point line is the step response for the system under the fixed-parameter PSS control.

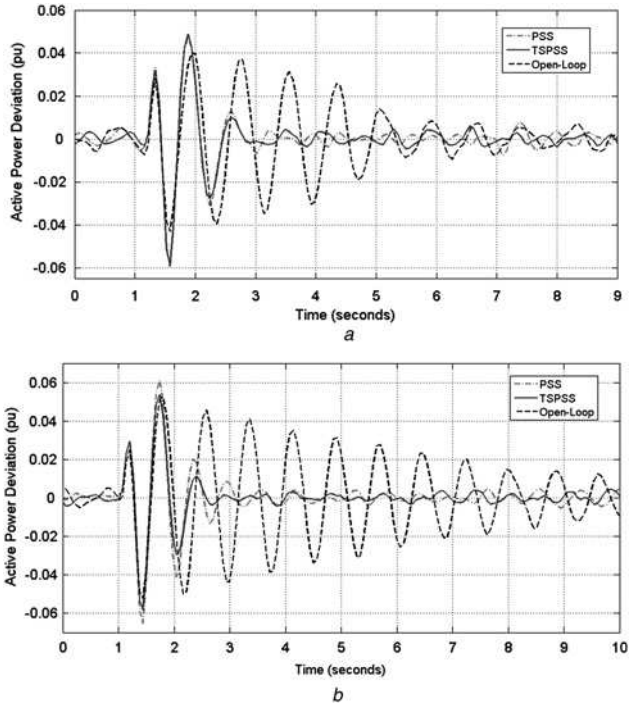

Fig. 9 *Step response at the operating points P_{T0} = {0.60, 0.70} pu and (with $V_{T0} = 1.000$ pu, $Q_{T0} \simeq 0.00$ pu), for the system with TSPSS (solid line) and fixed-parameter PSS (dashed-point line)*

It can be observed, from Figs. 9*a* and *b*, that while both controllers were able to provide sufficient damping for the dominant oscillation, the performance of the fixed-parameter PSS was sensibly degraded as the active power generation was increased. The TSPSS damping controller, in turn, presented a near constant performance for both operating conditions, showing an improved robustness, with respect to the fixed PSS, for varying operation conditions.

To quantitatively assess the performance of both damping controllers, TSPSS and fixed-parameter PSS, the step response tests were performed at operating points $P_{T0} = \{0.20, 0.40, 0.50, 0.6, 0.70\}$, and the following integral of the square error (ISE) performance indices were calculated for assessing the error and the control effort performance for the PSS and the TSPSS controllers: $J(e) = \int_0^t e^2(t)\mathrm{d}t \cong \sum_{k=0}^{N} (\Delta P_T(k))^2$ and $J(u) = \int_0^t u^2(t)\mathrm{d}t \cong$

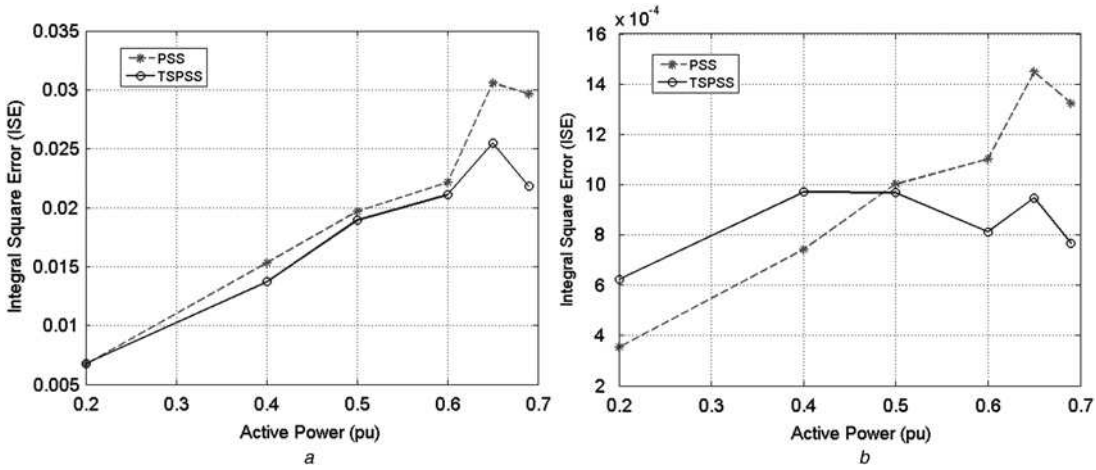

Fig. 10 *ISE performance indices as a function of the active power generation level*

$\sum_{k=1}^{N}(u(k))^2$, where $\Delta P_T(k)$ and $u(k)$ are, respectively, the measurements of the active power deviation and the corresponding effort control signal (from PSS or from TSPSS), at sample instant k.

Fig. 10*a* presents the $J(e)$ ISE index for the TSPSS controller (solid line) and for the fixed-parameter PSS (dashed line), as a function of the active power generation level. It can be seen that the TSPSS controller had ISE values smaller than those obtained by the fixed-parameter PSS controller for all sets of tested operating conditions. Also, it can be seen, from Fig. 10*a*, that the improved performance of the TSPSS, concerning the fixed-parameter PSS controller, becomes more evident as the level of active power generation was increased. This result shows the improved performance and the robustness of the TSPSS controller against varying operating conditions.

Fig. 10*b* shows the corresponding ISE index for the control effort for both controllers: TSPSS and fixed-parameter PSS. It can be observed that the ISE for the control effort of the TSPSS controller was less sensitive for varying operating condition than the ISE for the control effort of fixed-parameter PSS, keeping a near uniform ISE level as the active power generation is varied from low to high levels. Also, from Fig. 10*b* it can be seen that the TSPSS controller had a control effort smaller than the control effort of fixed-parameter PSS for operating conditions above 0.5 pu. Therefore, if compared with a fixed-parameter PSS, the developed TSPSS controller had an improved performance at high generation levels.

5 TSPSS field tests in a large power plant

Additional experimental tests were performed in a large generator system, at Tucuruí hydroelectric power plant (THPP). THPP is a very important power plant of the Brazilian interconnected power system (IPS). The power plant is made up of a set of 23 generating units (12 350 MVA and 11 375 MVA generating units), adding up to a total maximum generation capacity of 8325 MVA. The synchronous machines are equipped with fast thyristor-based excitation systems along with high-gain AVR. Each generating unit is equipped with a fixed-parameter PSS tuned to damp inter-area electromechanical modes observed in the large IPS.

For the field tests presented in this section, the target electromechanical oscillation mode was a dominant intra-plant oscillation mode observed from active power measurements taken at synchronous machine terminals. Field measurements confirmed that the dominant oscillating mode has a frequency around 1.5 Hz, originating from the interaction among the generating units of the power plant.

In this work, the inter-area modes were not addressed because, according to the Brazilian system operator [16], these modes are already well damped by a large set of coordinated PSS controllers located at strategic points of the IPS. Owing to the importance of THPP to the Brazilian IPS operation, there have been a lot of previous studies [16] performed by ONS (Operador Nacional do Sistema, an organisation responsible for assuring the safe operation of the Brazilian IPS), showing that the dominant mode of THPP against the external IPS is in the range of [0.53, 0.71] Hz for all operating conditions. Therefore, based on practical knowledge about the plant, the engineers have classified the observed 1.5 Hz oscillation mode as an intra-plant mode. The performance tests of the developed TSPSS were carried out on a 350 MVA generating unit of the Tucuruí Power Plant. To comply with operational safety restrictions, as well as the level of authorisation permitted by the Brazilian National System Operator (ONS), the tests were carried out in only one of the generating units of the

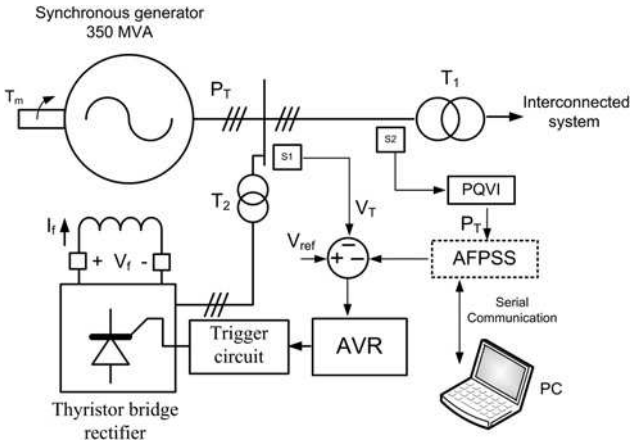

Fig. 11 *Simplified scheme of the connections between the digital PSS and the machine*

doi: 10.1049/iet-gtd.2013.0099

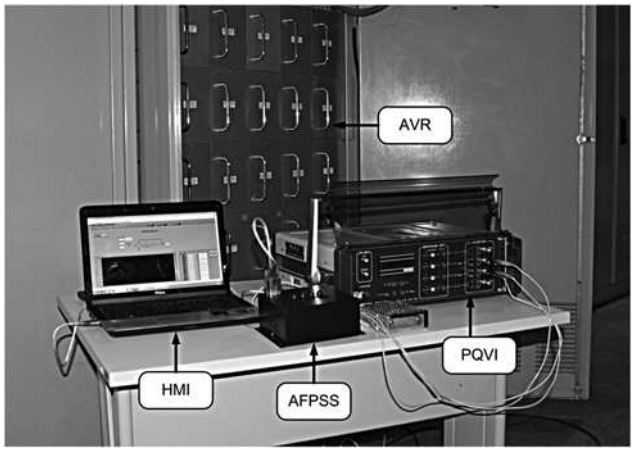

Fig. 12 *Electronic instrumentation used during field tests*

Tucuruí Power Plant. Therefore, generating unit #8 was selected for the field tests (Fig. 11).

5.1 Experimental identification of local models

To capture the dynamic information present in the collected dataset, the system was excited by adding a very low-amplitude PRBS test signal to the voltage reference of the AVR controller of a 350 MVA generating unit, by using the experimental scheme shown in Fig. 11. The PRBS test signal was designed to excite the range of frequencies of the electromechanical oscillation modes in electric power systems (usually in the range from 0.2 to 3.0 Hz, approximately). A value of 0.012 pu of the nominal reference value of the AVR controller was chosen for the PRBS test signal. The PRBS sequence was generated in order to excite uniformly the system modes in the band 0.02–5.5 Hz, which contains the natural frequency of the dominant electromechanical oscillation mode observed in the generating unit (~1.6 Hz).

During the evaluation tests, the plant was operating at around 74% of its nominal capacity, because of the current level of water in the reservoir. For this low head, the maximum and the minimum operational values of active power were around 0.74 pu (260 MW) and 0.625 pu (218 MW), respectively. The maximum value was limited by the maximum turbine output power (determined by turbine efficiency), and the minimum value was limited by the cavitation region of the hydraulic turbine (below 0.57 pu), which is not an allowed operating region. During the field tests, the conventional PSS of generating unit #8 was turned off, whereas the PSSs of the remaining plant generating

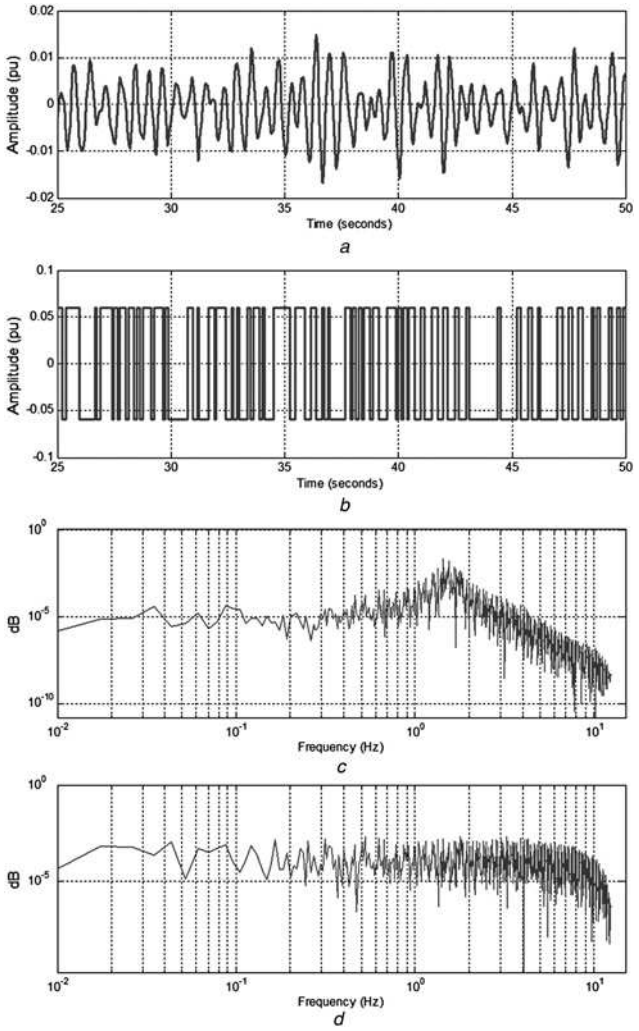

Fig. 13 *Experimental identification of local models*

a Output
b Input
c Data collected in field tests
d Respective spectrum

Table 6 Operational conditions of the identified models

	$Q = -0.2$ (negative)	$Q = 0.0$ (zero)	$Q = +0.2$ (positive)
$P = 0.75$ (high)	model P11	model P12	model P13
$P = 0.68$ (medium)	model P21	model P22	model P23
$P = 0.625$ (low)	model P31	model P32	model P33

Table 7 Values of the parameters of the nine identified linear models ($T_s = 50$ ms)

Local ARX models	a_1	a_2	a_3	a_4	b_0	b_1	b_2	b_3
11	−2.13639	1.67609	−0.44657	0.032673	0.002136	0.008460	−0.003179	−0.009508
12	−2.09560	1.63299	−0.429271	0.037391	0.001998	0.007586	−0.003005	−0.008973
13	−2.06168	1.57071	−0.36966	0.014087	0.014087	0.007128	−0.00289	−0.008463
21	−1.98614	1.30519	−0.12339	−0.06317	0.001432	0.00961	−0.002128	−0.011009
22	−2.01490	1.44659	−0.28098	0.00065	0.001987	0.0075653	−0.00196	−0.009643
23	−2.06857	1.58643	−0.38495	0.019414	0.001869	0.006860	−0.002847	−0.008026
31	−2.10662	1.59826	−0.39480	0.027353	0.0017716	0.008268	−0.002351	−0.009501
32	−2.008958	1.40979	−0.232311	−0.022863	0.001616	0.0076421	−0.001696	−0.009686
33	−2.071433	1.579434	−0.377348	0.017153	0.001692	0.006774	−0.002506	−0.008263

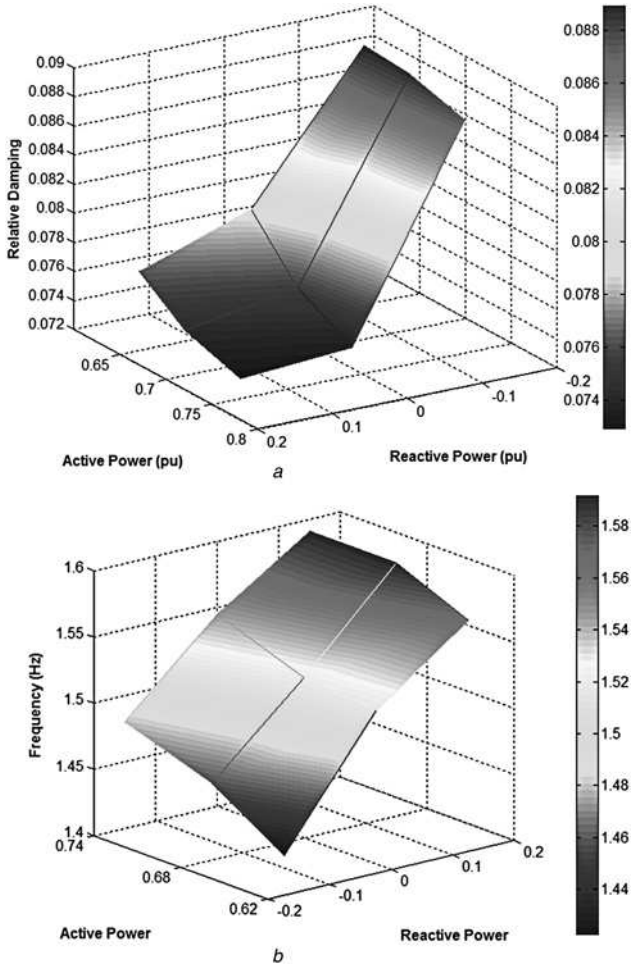

Fig. 14 *Estimated values for the*

a Damping
b Frequency of the oscillating mode as a function of the test operating conditions

units were all kept activated. The electronic instrumentation used in the field tests was mounted on the generating unit AVR cabinet, as shown in Fig. 12.

According to the physical limitations of the plant, the operating region in the $P \times Q$ plane (generator capability curve) was segmented into nine regions, corresponding to three levels of active and reactive power operating conditions, as shown in Table 6. For each $P \times Q$ subregion, a corresponding linear local ARX model was identified. The local model is representative of the system dynamics around the respective $P \times Q$ operating region. The parameters of the identified ARX models were then utilised for the design of the TSPSS control.

The input and output data collected for a specific operating point (model P11 in the Table 7) are shown in Figs. 13*b* and *a*, respectively. The input is the PRBS signal applied to the AVR reference, and the output is the active power deviation signal collected by using a PQVI transducer piece of equipment. For data acquisition and control, a fixed sampling time, T_s, of 0.05 s, was used during all the tests carried out.

The spectra for output and input measured signals are shown in Figs. 13*c* and *d*, respectively. As can been seen, the spectrum of the input PRBS signal (Fig. 13*d*), is approximately uniform in the range of the electromechanical modes. In the frequency spectrum for the output signal (Fig. 13*c*), in turn, the presence of a peak

Table 8 List of the dominant poles of the nine identified linear models

Operating points	Dominant poles	Damping	Frequency, Hz
P11	8.59e-001 + 4.29e-001i	0.0875	1.4801
P12	8.54e-001 + 4.49e-001i	0.0735	1.5453
P13	8.46e-001 + 4.63e-001i	0.0729	1.5915
P21	8.62e-001 + 4.23e-001i	0.0886	1.4578
P22	8.57e-001 + 4.42e-001i	0.0755	1.52152
P23	8.46e-001 + 4.61e-001i	0.0742	1.5915
P31	8.67e-001 + 4.14e-001i	0.0889	1.42284
P32	8.56e-001 + 4.40e-001i	0.0792	1.51674
P33	8.49e-001 + 4.54e-001i	0.0765	1.56767

located around the frequency value of 1.6 Hz is clear, which corresponds to the observed dominant intra-plant electromechanical oscillation mode. As can be seen, the intra-plant mode shows reduced damping. Therefore it is advisable to design the TSPSS controller in a way that increases the damping of the dominant electromechanical mode.

Repeating the test for all $l = 9$ operating points, the parameters of the local model polynomials $A^{(l)}(q^{-1})$ and $B^{(l)}(q^{-1})$ were estimated from collected input/output data, by using a non-recursive least squares algorithm. For all identified local ARX models, the polynomials $A(q^{-1})$ and $B(q^{-1})$ order was $n_A = n_B = 4$. The values of the identified parameters are provided in Table 7 (the sampling time used, T_s, was 0.05 s). The identified models were validated by comparing model output and the measured collected data, as well as correlation tests of the residuals. In Fig. 14*a*, the behaviour for the estimated values of the relative damping as a function of the operating conditions (Table 8) is shown. It can be observed (see Fig. 14*a*) that the value of the damping of the dominant electromechanical mode becomes reduced for operating conditions, where the generator is supplying reactive power to the grid. From Fig. 14*b*, it can be observed that the frequency of the oscillation mode increases as the reactive power generation increases.

5.2 Design and field tests of the TSPSS

After concluding the identification of the nine local models representative of system dynamics in different operating conditions, the next step was to design a digital controller for each local model. These controllers will comprise the local controller network of the TSPSS. The local controllers were designed by using the pole-shifting method, already presented in Section 2.2. All the local controllers were designed to provide a desired damping of $\xi_d = 0.3$ for the observed dominant electromechanical mode of 1.6 Hz. The values of the parameters for the calculated local controllers are shown in Table 9.

For the adjustment of the fuzzy supervisor, the partitioning of operating variables P and Q in fuzzy sets was performed according to Section 2.4 of this paper. To qualitatively characterise the operation variable P, three fuzzy sets were chosen, the centres of which are located at values of $P_{low} = 0.62$ pu, $P_{medium} = 0.68$ and $P_{high} = 0.75$, respectively. On the other hand, to qualitatively characterise the operation variable Q, three fuzzy sets having their centres at values of $Q_{negative} = -0.2$ pu, $Q_{zero} = 0.0$ pu and $Q_{positive} = 0.2$ pu, were selected.

doi: 10.1049/iet-gtd.2013.0099

Table 9 Coefficients of the local controllers

Local controller number	r_0	r_1	r_2	r_3	s_1	s_2	s_3
11	12.6659	−11.8435	3.1540	−0.2279	0.1739	−0.0107	−0.0663
12	15.0323	−13.7243	3.6513	−0.3142	0.1881	−0.0146	−0.0754
13	16.3208	−14.7454	3.4194	−0.1295	0.1905	−0.0151	−0.0778
21	11.7960	−9.2589	0.7225	0.4123	0.1663	0.00054	−0.0718
22	14.7466	−12.4952	2.4019	−0.0055	0.1757	−0.0120	−0.0824
23	16.9546	−15.4391	3.7188	−0.1862	0.1893	−0.0167	−0.0770
31	12.9490	−11.6124	2.8916	−0.1989	0.1666	−0.0101	−0.0691
32	14.6264	−2.1651	1.8984	0.1891	0.17693	−0.00411	−0.0801
33	16.4191	−14.6549	3.4400	−0.1550	0.1881	−0.0088	−0.0747

Table 10 Values of damping and frequency of the dominant poles of the models identified in closed loop

Test	*P*, pu	*Q*, pu	Case	Damping	Frequency, Hz
T1	0.7	0.18	without PSS	0.0737	1.59
T1	0.7	0.18	fixed PSS	0.270	1.66
T1	0.7	0.18	TSPSS	0.290	1.656
T2	0.687	0.035	without PSS	0.0774	1.5366
T2	0.687	0.035	fixed PSS	0.287	1.5812
T2	0.687	0.035	TSPSS	0.301	1.5843

After the design of local controllers and tuning the fuzzy supervisor, the performance of the TSPSS was evaluated by performing tests under various operating conditions. To compare the closed-loop performance of the system, at each test point, the tests were carried out in three different situations: (i) without using PSS, (ii) using a fixed-parameter PSS and (iii) using the TSPSS. Among the nine local controllers, the central one was chosen as the fixed-parameter PSS. This fixed PSS was tuned in the central operational condition (having reactive power 'zero' and active power 'medium').

Table 10 presents the values of damping and natural frequency of the dominant poles of the models identified in two operational conditions (named T1 and T2). It can be observed that under control of the TSPSS, the damping of the dominant oscillation mode is closer to the desired value of approximately $\xi_d = 0.3$, as required. On the other hand, it can be observed from Table 10 that there is a reduction in the estimated damping value for operating conditions other than that used for the fixed PSS design. This result shows that the system equipped with the TSPSS was able to adjust its parameters in order to keep the performance of the system at the desired value, even with variations in the plant's operating conditions.

Fig. 15 shows the step response from the system at test point 1. As can be seen, the low-damped electromechanical

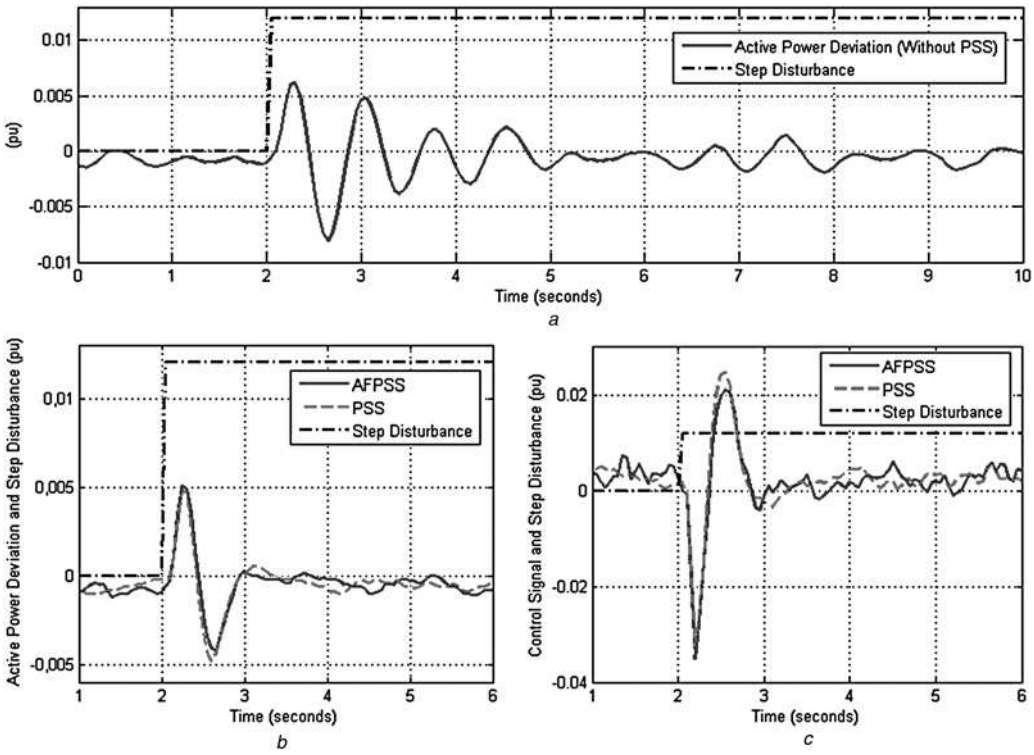

Fig. 15 *Step response from the system*

a Without PSS
b With fixed PSS
c With TSPSS

oscillation mode can be observed in the active power deviation signal, during the step response for the system without PSS, as presented in Fig. 15*a*. A comparison between the system response with the fixed-parameter PSS and the system response with the TSPSS is shown in Fig. 15*b*. It can be observed that for the tests carried out in the plant, the performance of both fixed and TSPSS controllers were almost the same. However, by analysing the control effort signals for both the PSS and TSPSS controllers (Fig. 15*c*), it can be observed that the control signal of the system having fixed PSS shows a peak amplitude greater than the peak amplitude of the TSPSS control effort signal. Therefore, even though conducting field tests under a large set of operational conditions was not possible, the reduced control effort of the TSPSS controller indicates its improved performance.

6 Conclusions

In this paper, the design and experimental tests of an adaptive fuzzy-based PSS, along with its performance on damping dominant electromechanical oscillations in power systems, were addressed. The TSPSS performance was assessed in laboratory tests by using a reduced-scale power system, as well as by field tests in a large power plant of the interconnected Brazilian power system. The TSPSS controller presented a good performance by providing sufficient damping for the dominant electromechanical oscillation, at varying operating conditions. Laboratory test results (Section 4) showed that the TSPSS controller was able to keep its performance almost uniform for varying operating conditions, wheras the corresponding performance of a fixed-parameter PSS was considerably degraded by varying operating conditions. The improved performance was obtained without using an excessive control effort concerning control effort of a fixed-parameter PSS.

The field tests carried out in a large-unit generating system showed that the observed dominant intra-plant oscillation mode was efficiently damped. It is worth emphasising that an improved performance could be obtained by increasing the number of local controllers. However, this has the drawback of increasing the controller's complexity. The identification methodology applied to determine local models was shown to be very efficient in the field tests, allowing for the identification of good performance models for controller design purposes. Owing to power plant operation constraints and the availability of generating units for the execution of field tests, the time intervals permitted to perform the field tests were usually very short. The experimental results from both laboratory and large power plant tests indicate the superior performance obtained by the proposed TSPSS controller.

The small performance difference observed between the fixed PSS and TSPSS may be because of similar operating conditions during the tests, in particular for the field tests carried out at the large power plant, because of some plant operational restrictions such as cavitations phenomena and level of water in the reservoir. It is expected that, by repeating the tests for a wider range of operating conditions, the improved performance of the controller would be much more pronounced. The authors are now trying to obtain, from the utility, an authorisation for performing additional field tests for a wider range of operating conditions, but this can be a long-term process.

Beside the changes on the operating conditions because of the changes in the generator loading, the system is also subject to topological changes, such as operating with a reduced number of transmission lines, for instance. Therefore a kind of adaptive scheme based on recursive on-line estimation should be added to current fuzzy strategy. This subject is to be investigated and the results will be reported in the future paper.

7 Acknowledgment

The authors acknowledge the support of ELETRONORTE, through the R&D project number 4500063758 (2010), and from CNPq (The Brazilian National Research Council).

8 References

1 Rogers, G.J.: 'The application of power system stabilizers to a multigenerator plant', *IEEE Trans. Power Syst.*, 2000, **15**, (1), pp. 350–355
2 Crenshaw, M.L., Cutler, J.M., Wright, G.F., Reid, Jr., W.J.: 'Power system stabilizer application in a two-unit plant analytical studies and field tests', *IEEE Trans. Power Appar. Syst.*, 1983, **2**, pp. 267–274
3 Araújo, C.S., Castro, J.C.: 'Application of power system stabilizers in a plant with identical units'. IEE Proc. C, 1991, 138, (1), pp. 11–18
4 Nogueira, F.G., Barreiros, J.A.L., Barra, Jr., W., da Costa Jr. C.T., Ferreira, A.M.D.: 'Development and field tests of a damping controller to mitigate electromechanical oscillations on large diesel generating units', *Electr. Power Syst. Res.*, 2011, **81**, (2), pp. 725–732
5 Sena, J.A.S., Fonseca, M.C.P., Di Paolo, I., Barra, Jr., W., Barreiros, J.A. L., da Costa, Jr., C.T., Nogueira, F.G.: 'An object-oriented framework applied to the study of electromechanical oscillations at Tucuruí hydroelectric power plant', *Electr. Power Syst. Res.*, 2011, **81**, (12), pp. 2081–2087
6 Kamua, I., Grondin, R., Trudel, G.: 'IEEE PSS2B versus PSS4B: the limits of performance of modern power system stabilizers', *IEEE Trans. Power Syst.*, 2005, **20**, (2), pp. 903–915
7 Lim, C.M., Hiyama, T.: 'Application of a self-tuning control scheme to a power system with multi-mode oscillations', *Electr. Power Syst. Res.*, 1992, **24**, (2), pp. 91–98
8 Ferreira, A.M.D., Barreiros, J.A.L., Barra, Jr., W., de Souza, J.R.B.: 'A robust adaptive LQG/LTR TCSC controller applied to damp power system oscillations', *Electr. Power Syst. Res.*, 2007, **77**, (8), pp. 956–964
9 Bandal, V., Bandyopadhyay, B.: 'Robust decentralised output feedback sliding mode control technique-based power system stabiliser (PSS) for multimachine power system', *IET Control Theory Appl.*, 2007, **1**, (5), pp. 1512–1522
10 De Oliveira, R.V., Ramos, R.A., Bretas, N.G.: 'Using the output energy as performance index in the design of damping controllers for power systems', *IET Control Theory Appl.*, 2007, **1**, (5), pp. 1191–1199
11 Dobrescu, M., Kamwa, I.: 'A new fuzzy logic power system stabilizer performances'. Proc. IEEE PES, Power Conf. and Exposition, 2004, vol. 2, pp. 1056–1061
12 Barra, Jr., W., Barreiros, J.A.L., da Costa, Jr., C.T., Ferreira, A.M.D.: 'Fuzzy control applied to improve the dynamic stability of electrical power systems', *Controle Autom.*, 2005, **16**, (2), pp. 173–186 (in Portuguese)
13 Johansen, T.A., Hunt, K.J., Petersen, I.: 'Gain scheduled control of a solar power plant', *Control. Eng. Pract.*, 2000, **8**, pp. 1011–1022
14 Ljung, L.: 'System identification: theory for the user' (University of Linköping Sweden, Prentice-Hall, Englewood Cliffs, New Jersey, 1987, 2nd edn.)
15 Landau, I.D., Zito, G.: 'Digital control systems: design, identification and implementation' (Springer, 2006, 1st edn.)
16 Operador Nacional do Sistema, 'Optimization of controllers of the interconnected national system'. Technical report 'RE 3/121/2002', 2002, (in Portuguese)